Thermo-mechanical and photo-luminescence properties of micro-actuators made of liquid crystal elastomers with cyano-oligo(p -phenylene vinylene) crosslinking bridges

Bin Ni, Hui Chen, Mengxue Zhang, Patrick Keller, Michael Tatoulian, Min-Hui Li

Journal Name

ARTICLE

Thermo-mechanical and photo-luminescence properties of micro-actuators made of liquid crystal elastomers with cyano-oligo(p-phenylene vinylene) crosslinking bridges†

eceived 00th January 20xx,
Accepted 00th January 20xx

DOI: 10.1039/x0xx00000x

www.rsc.org/

Bin Ni, ‡,[a] Hui Chen, ‡,[a,b] Mengxue Zhang,[a] Patrick Keller,*,[c] Michael Tatoulian,*,[a] and Min-Hui Li*,[a,b]

Nematic liquid crystal elastomers (LCEs) micropillars with reversible thermomechanical deformations and photo luminescence (PL) intensity variations were successfully fabricated by introducing a cyano-oligo(p-phenylene vinylene) dye as chemical crosslinker. The PL intensity of the micropillars decreased and increased reversibly during the thermal-deformation process. We studied in detail the possible factors that influence the PL intensity variations of the micropillars, including temperature variation, contraction/extension and phase transition. The dye molecules mainly kept the "monomer" state in the micropillars during the thermo-activated deformation. It was found that the phase transition from nematic to isotropic of the LCEs played the major role in the PL intensity variations. This kind of micropillars may have potential application as fluorescent soft sensors and actuators.

Introduction

Liquid crystal elastomers (LCEs) are a type of smart materials, which have attracted increasing research interests in recent years owing to their potential applications in smart sensors[1], high-frequency oscillators[2,3], microfluidic device[4,5], gas separation membranes[6], artificial muscles[7, 8], and so on. LCEs can be seen as liquid crystalline polymers (LCP) with slightly crosslinked polymer chains, which show both the anisotropic orientation characteristic of liquid crystals and the rubbery elasticity of polymer networks[9]. The molecular organization in the different phases has a great influence on the properties of the LCEs. In the LC phase, the conformation of the macromolecular backbone is coupled with the orientational order of the mesogen units. For example, in the nematic phase, the orientated mesogens force the polymer chains to stretch along the direction of the orientation [10-12]. However, when the transition from nematic to isotropic phase takes place, the orientational order is lost; consequently, the polymer chains can go back to the usual random coil conformation. This conformational change induced by nematic to isotropic phase transition causes the macroscopic shape change of LCEs. Meanwhile, thanks to the crosslinked network, the orientational order can be restored to its original state, which endows LCEs with the reversible shape-memory properties. Moreover, the shape variation of LCEs can be produced by using various stimuli, such as light illumination, heating, electric and magnetic fields etc., giving the opportunity to develop thermo-responsive[13-21], photo-responsive[22-29], and electro-responsive[30-33] smart LCEs.

Luminescent smart materials responsive to external stimulus, like mechanical stress[34-36] or temperature[37], have gained increased attention since they might have applications in sensitive sensors[38], organic light emitting diodes (OLEDs)[35] and security printing[39]. Weder[40, 41] introduced dye molecules, cyano-p-phenylene vinylene (cyano-OPV) derivatives, as the dopant compound into linear low-density polyethylene (LLDPE) to make stress-sensitive luminescent materials. The tensile deformation of the LLDPE materials forced the cyano-OPV molecules to change from the "excimer" state to the "monomer" state to realize the chromic properties. This kind of deformation-induced fluorescence color change could be used as strain sensors in polymer objects. In a previous study, one of us[42] mixed similar cyano-OPV molecule (1,4-bis(α-cyano-4-methoxystyryl)benzene) as the dopant with a nematic LCE. Upon the thermomechanical shape change of LCE, they observed, however, only a diminution of the fluorescence

[a] *Chimie ParisTech, PSL University Paris, CNRS, Institut de Recherche de Chimie Paris, UMR8247, 11 rue Pierre et Marie Curie, 75005 Paris, France.*
Email: min-hui.li@chimieparistech.psl.eu;
michael.tatoulian@chimieparistech.psl.eu
[b] *Beijing Advanced Innovation Center for Soft Matter Science and Engineering, Beijing University of Chemical Technology, 15 North Third Ring Road, Chaoyang District, 100029 Beijing, China.*
[c] *Institut Curie, Laboratoire Physico-Chimie Curie, UMR168, 11 rue Pierre et Marie Curie, 75005 Paris, France. Email: patrick.keller@curie.fr*

† Electronic Supplementary Information (ESI) available: Synthetic routes, MS and NMR spectra of β-cyano-OPV; DSC curves of β-cyano-OPV; Fluorescence images of β-cyano-OPV powders. Photo-isomerization of β-cyano-OPV in solution and the stability of its isomers. Effect of the photo-isomerization on the optical properties. Complemental data of thermomechanical and photo-luminescence properties and DSC curves of LCE micropillars with different contents of β-cyano-OPV. Complemental data of factors that might affect the PL intensity of LCE micropillars. See DOI: 10.1039/x0xx00000x.

‡ These authors contributed equally to this work.

intensity during the contraction of the LCE. As a matter of fact, in the systems where shape changes co-exist with temperature variations and phase transitions, other physical phenomena could also affect the PL intensity variations. In particular, the influence of phase transitions was already reported in ceramic[43], gels[44], and liquid crystal[45]. G. Meier[45] et al discovered that the quantum yield of fluorescence of a dye dissolved in a LC mesophase changed dramatically at the phase transition from the nematic to the isotropic phase.

Following our previous work on fluorescent LCEs[42], we prepared here new nematic LCEs by introducing the fluorescent cyano-OPV dye(Scheme 1, β-cyano-OPV) as the crosslinker which was thus connected chemically to the LCEs. The fluorescent nematic LCEs were prepared in the form of micropillars with different crosslinking degrees and different contents of dye crosslinker cyano-OPV in the whole concentration of crosslinkers. Those new micropillars gave us the opportunity to study in detail the relationships between the PL properties and each potential factor influencing the PL intensity, such as temperature change, contraction and extension, and phase transition. The monodomain LCE micropillars were fabricated using β-cyano-OPV ((((1Z,1'Z)-1,4-phenylenebis(1-cyanoethene-2,1-diyl))bis(4,1-phenylene))bis(oxy))bis(hexane-6,1-diyl) bis(2-methylacrylate), (see Scheme 1) as the dye crosslinker associated with a flexible and non-fluorescent crosslinker and MA444 ((4-methacryloyloxy)butyl 2,5-di-(4'-butyloxybenzoyloxy)benzoate, see Scheme 2) as the nematic monomer, by the previously described magnetic alignment method[14]. Then the PL intensity variations and the thermomechanical properties of these micropillars were investigated. It was found that the phase transition from nematic to isotropic of the LCEs played the major role in the PL intensity variations.

Results and discussion

Synthesis of the dye crosslinker and preparation of LCE micropillars

We synthesized the dye crosslinker β-cyano-OPV according to the Scheme 1. The details of the syntheses and characterization are described in the Electronic Supplementary Information(ESI).

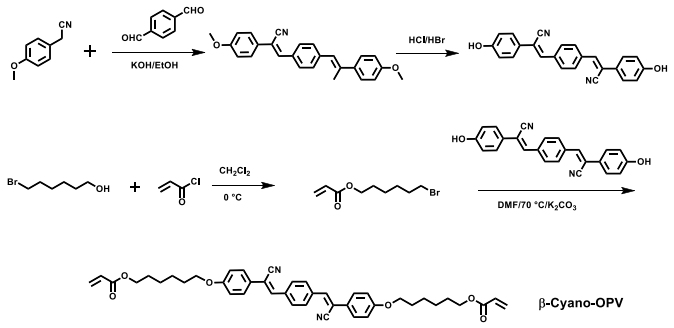

Scheme 1. Synthetic route of the dye crosslinker β-cyano-OPV (β-cyano-OPV).

The phase behaviour of the β-cyano-OPV was studied by differential scanning calorimetry (DSC) and polarizing optical microscopy (POM). The β-cyano-OPV exhibits two endothermic transitions at 130 °C and 146 °C according to DSC measurement (Figure S3 in SI). A complementary analysis by POM helped to identify the phase transition at 130°C as the crystal-to-nematic phase transition, and the one at 146°C as the nematic-to-isotropic phase transition.

Then the micron-sized LCE pillars were fabricated by photo-polymerization under magnetic field alignment as previously described[14], using the mixtures of LC monomer (MA444), photo-initiator (2-benzyl-2-(dimethylamino)-4'-morpholinobutyrophenone) and a flexible crosslinker (1,6-hexanediol dimethacrylate) (see Scheme 2) together with the dye crosslinker (β-cyano-OPV). The monomer MA444 was synthesized according to the procedure already published. The phase sequence of MA444 are Cr 83 Iso on heating and Iso79 N 60 Cr on cooling[46]. The concentration of the photoinitiator was kept at 2 mol%, while various concentrations of crosslinkers were used. First on keeping the whole crosslinkers concentration at 10 mol%, the concentration of the β-cyano-OPV was varied from 0.5 mol% to 5 mol% in order to study the effect of the dye concentration. Then on keeping the concentration of β-cyano-OPV at 1 mol%, LCEs with different whole crosslinker concentrations (10 mol% and 35 mol%) were prepared in order to compare PL properties of slightly and highly crosslinked LCEs. The phase transition of each mixture for micropillar preparation was checked beforehand to ensure that the photo-polymerization occurred in aligned nematic phase.

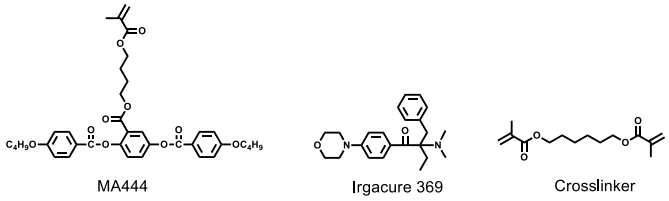

Scheme 2. Chemical structures of the monomer MA444, the photo-initiator (Irgacure 369) and the flexible crosslinker.

Fluorescence properties of the dye crosslinker (β-cyano-OPV)

The PL properties of the cyano-OPV derivatives are sensitive to their "environment", for example in solution or in solid-state (amorphous or crystalline) as reported by Weder et al[41, 42]. The authors linked this sensitivity to the existence of "monomer state" versus "excimer state" for the dye molecules when they were "dispersed" versus "aggregated". Therefore, it is important to characterize the fluorescence properties of the β-cyano-OPV in different environments, i.e., in solution, in the LCE micropillars and in pure state.

Fig 1 shows the PL excitation and emission spectra of the β-cyano-OPV in different environments. Fluorescence excitation spectra of the β-cyano-OPV, both in dichloromethane solution and in the micropillar, are presented in Fig 1a and 1b, respectively. The maximum excitation is around 396 nm in solution, while in the micropillar, the excitation curve broadens and red-shifts with a maximum around 420 nm. As

for the fluorescence emission of the β-cyano-OPV, Fig 1c and 1d show very similar emission spectra with maximum around 460 - 490 nm in the CH_2Cl_2 solution and in the micropillars. This observation indicates a similar molecular organization of the dye molecules both in solution and within the elastomer. Since the β-cyano-OPV is well dissolved in the dichloromethane, the dye crosslinker is in the monomeric state (unimer) in solution. We can then deduce that the dye crosslinker is also in the monomeric state in the LCE micropillars. Finally, we checked the fluorescence emission of the pure β-cyano-OPV in the solid state. As shown in Fig 1e, a sharp emission peak was observed at 515 nm, together with a shoulder emission at 550 nm, which is a typical emission spectrum for the excimer emission as previously ascribed in the literature[41]. With naked eyes, we observed that the β-cyano-OPV in solid state exhibited a strong green-yellow fluorescence under UV light irradiation (Fig S4). This fluorescence was associated with the presence of excimers as described by Weder et al[41]. The sharp contrast between the emission spectra of the dye crosslinker in pure solid state and in LCE micropillars confirmed again that the dye crosslinker molecules are in the monomeric state both in the LCE micropillars.

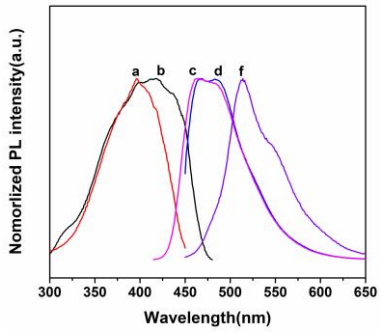

Fig. 1 The PL excitation and emission spectra of the β-cyano-OPV in different environments. (a) The excitation spectrum in CH_2Cl_2 solution (10^{-5} mol/L). (b) The excitation spectrum in micropillars. (c) The emission spectrum in CH_2Cl_2 solution under the excitation light of 396 nm. (d) The emission spectrum in micropillars under with the excitation light of 420 nm. (e) The emission spectrum in the pure solid state with the excitation light of 420 nm.

Thermomechanical properties of the LCE micropillars

After the photopolymerization, optical microscopy, scanning electronic microscopy (SEM) and fluorescence microscopy were used to observe the regular array of micropillars and separated micropillars. As shown in Fig 2a, the optical microscopy image showed the regular array of micropillars on a large scale, demonstrating that the method was suitable for preparation of micropillars with a high efficiency and accuracy. SEM image of the micropillars array is presented in Fig 2b, which further confirms the structures. Fig 2c and 2d show the separated micropillars under POM without and with crossed polarizers, respectively. No obvious defects could be observed in the long axis of the micropillars in the Fig 2d, indicative of a relatively good alignment of the nematic mesophase. The regular array of micropillars and the separated micropillars were also observed by fluorescence microscopy under UV light excitation (365 nm) and blue light excitation (450 nm) as shown in Fig 2e, 2f, 2g and 2h, respectively. The LCE micropillar actuators exhibited a blue emission under UV excitation and a green emission under blue light excitation. The average length of the micropillars was measured to be around 70 micrometers from both the fluorescence images and optical images.

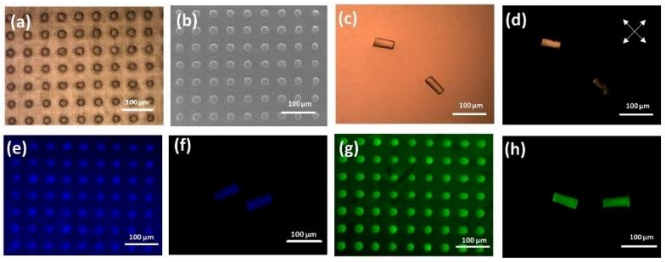

Fig. 2 Images of the LCE micropillars containing the β-cyano-OPV as crosslinker. (a): Optical microscopic image of the micropillars. (b): SEM image of the micropillars. (c): Separated micropillars observed under POM without crossed polarizers. (d): Separated micropillars under POM with crossed polarizers. (e) and (f): Fluorescence image of the micropillars excited by UV light of 365 nm. (g) and (h): Fluorescence image of the micropillars excited by blue light of 450 nm.

The thermally-induced actuation properties of the micropillars were investigated by measuring the micropillars lengths at different temperatures. Before this investigation, we first checked the thermo-stability of the LCE by TGA (see Figure S11C). The TGA showed that the LCE was very stable in the temperature range of our investigation (< 200°C). Micropillars were dispersed in low viscosity silicone oil on a clean glass slide in order to avoid friction between the actuators and the glass surface. The glass slide was kept on a heating stage under the optical microscope. Four different micropillars were prepared with various contents of the dye crosslinker (0.5 mol %, 1 mol %, 2 mol %, 5 mol % respectively) on keeping the whole crosslinkers concentration constant (10 mol%). As an example, the deformation of the micropillars with 1 mol % of dye crosslinker as a function of temperature is presented in Fig 3 (the others are presented in Fig S9 and S10). Fig 3a shows the thermally-induced spontaneous shape deformation behavior of the micropillars during a heating and cooling cycle between 25 °C and 100 °C. Upon heating at 100 °C, the length of micropillars reduced around 30%. Upon cooling, the length of micropillars recovered to their original value. Then we selected 10 separated micropillars to measure their lengths along the longitudinal direction when the temperature was varied from 25 °C to 100 °C and from 100°C back to 25 °C. The contraction and relaxation were characterized by L/ L_{iso} as a function of temperature as shown in Fig 3b, where L_{iso} is the minimum length of the micropillar in its isotropic state and L is the length of the micropillar at any given temperature. Contraction during the heating process was observed in the temperature range 70-85 °C, which corresponds to the nematic–isotropic transition temperature (T_{NI}) of the LCE samples (Fig S11). It is clear that the thermomechanical deformation mainly occurs at T_{NI} of the LCEs. On cooling back to 25 °C, pillars expanded and recovered the initial shape and

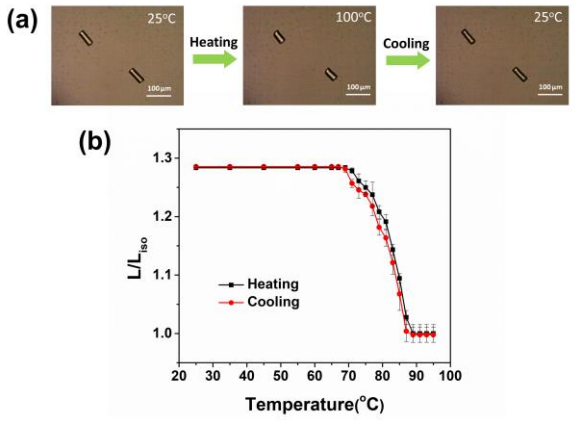

size. All these observations demonstrated that the micropillars have a fully reversible shape memory property.

Fig. 3 (a) The optical images of micropillars containing 1 mol % dye crosslinker at different temperatures. (b) The contraction and relaxation represented by L/L_{iso} along the long axis of these micropillars at heating and cooling process, 10 micropillars being analyzed. L_{iso} and L are the length of the micropillar in its isotropic state and at any given temperature, respectively.

In addition, the influence of the β-cyano-OPV content on the deformation properties was also investigated. As shown in Fig 4a, the contraction behaviours kept the same, but their extent L/L_{iso} decreased as the content of the dye crosslinker increased. This observation indicated probably the order parameters of the LC alignment decreased with the increase of β-cyano-OPV content in the crosslinking bridges. As a matter of fact, during the photopolymerization to prepare the LCE, the β-cyano-OPV dye could also absorb the UV light to undergo photoisomerizations (see ESI Section 3, Fig S5). The initial isomer Z/Z was rod-like and compatible to the nematic order, however the isomers Z/E and E/E produced under UV illumination had bent form and should play the role of impurities in the nematic system. Therefore, the order parameters of the LC alignment should decrease with the increase of content of isomers Z/E and E/E, which were proportional to the starting content of β-cyano-OPV crosslinker. To evaluate the content of possible isomers in the micropillars and their thermal stability, we used the β-cyano-OPV dye in solution in $CDCl_3$ or DMSO-D_6 (concentration = 10^{-4} mol/L) as model system, which was irradiated during different time until 30 min and then analysed by ^{1}H-NMR. Note that 30 min is the duration of photopolymerization. The details are presented in the ESI (Section 3). As shown in Table S1 and Fig S5 and S6, the study by ^{1}H NMR spectra indicated that the isomerization took place in β-cyano-OPV in solution after 30 min of UV irradiation. However, after keeping the irradiated β-cyano-OPV solution at room temperature for 30 days in dark or heating up to 110 °C for 10 min in dark, there is nearly no change in the positions and intensities of the ^{1}H NMR signals. That means that the isomerized structures are thermally stable. We extrapolated this conclusion to the possible isomers in the LCE micropillars. (We believe this is reasonable because the molecular mobility is lower in LCE than in solution). This indirectly indicated that the possible isomer structures existing

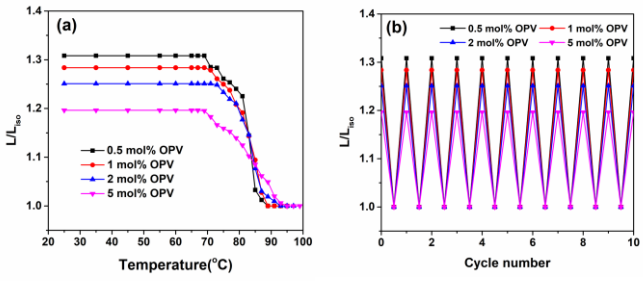

in the LCE micropillars will not be affected during the thermally-induced deformation process. This was actually

Fig. 4 (a) The deformation properties of the micropillars with different concentrations of β-cyano-OPV dye crosslinker. (b) The reversible thermal deformation of these micropillars within 10 heating and cooling cycles between 25 °C and 100 °C.

approved by the repeating cycles of the thermally-induced deformation as shown in Fig 4b. The contraction and recovery cycling processes were carried out from 25 °C (in nematic phase) to 100 °C (in isotropic phase) and back to 25 °C repeatedly for ten times. The thermally-induced deformation properties remained stable, which demonstrates the thermomechanical stability of these micropillars.

Photo-luminescence properties of the LCE micropillars

The fluorescence properties of the micropillars are induced by the fluorescent crosslinker β-cyano- OPV. The PL intensity evolution was studied during the heating and cooling cycle between 25 °C and 105 °C. Two different excitation wavelengths (UV light at 365 nm and blue light at 450 nm) were used for the micropillars in the fluorescence microscope. Under UV excitation, the micropillars emitted blue light, while under blue light excitation, the micropillars emitted green light (Fig 5a and 5d). The fluorescence intensity variations and pillars deformations at different temperatures (25 °C, 105 °C, 25 °C) are presented in Figure 5. When the LCE micropillars were heated to their isotropic phase, the PL intensity decreased, meanwhile the length contracted, as shown in Figure 5b and 5e. After cooling down to 25 °C, the PL intensities of the micropillars recovered to a certain extent. We then analysed the variations of the PL intensity and of the length of the micropillars (10 samples) as a function of the temperature with the aid of the ImageJ software, as described

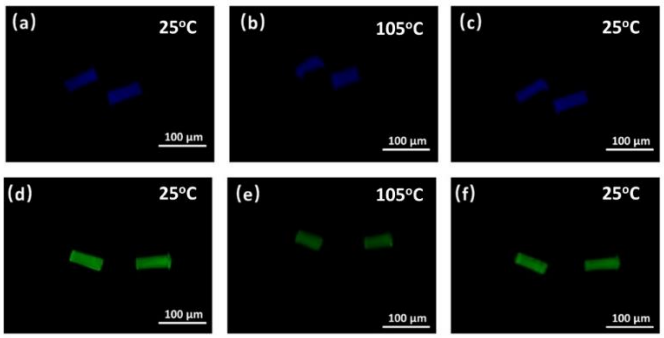

Fig. 5 Fluorescence images of LCE micropillars under different excitation lights and at different temperatures. (a), (b) and (c): Fluorescence images at 25 °C, 105 °C and 25 °C

under UV light excitation at 365 nm. (d), (e) and (f): Fluorescenc images at 25 °C, 105 °C and 25 °C under blue light excitation at 450 nm.

in the Experimental Section. Fig 6 shows the evolution of the PL intensity and the pillar deformation at different temperatures. With temperature increasing, the pillars contracted and the PL intensity decreased for both excitation wavelengths. When the temperature reached 80 – 100 °C upon heating, the PL intensity decreased sharply; upon cooling the PL intensity exhibited a fast recovery also within the 100 – 80 °C temperature range. These observations indicated that the PL intensity variation was related to the various phenomena occurring within this temperature range: the temperature change, the nematic-to-isotropic phase transition and the deformation of the micropillars. Fig 6 shows the data of the LCE micropillars containing 1 mol% β-cyano-OPV crosslinker. Fig S12-S17 show the data of the LCE micropillars with other contents of β-cyano-OPV crosslinker (0.5, 2 and 5 mol%). At this stage, we would like to emphasize that the various β-cyano-OPV concentrations used in the preparation of the micropillars did not influence the global tendency of PL intensity variations.

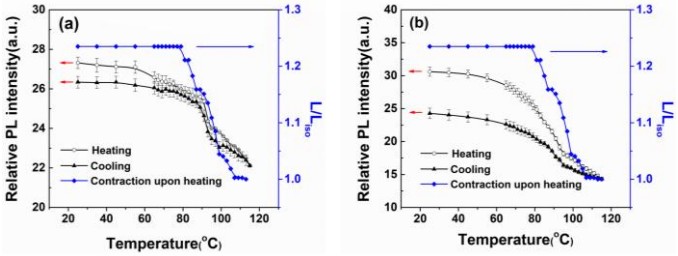

Fig. 6 The variation of fluorescence intensity and the ratio of contraction of the micropillars containing 1 mol% β-cyano-OPV crosslinker, as a function of temperature during the heating and cooling process. (a) under UV light excitation at 365 nm. (b) under blue light excitation at 450 nm.

Analyses of factors that might affect the PL intensity of LCE micropillars

The potential factors which might affect the PL intensity variations during the heating and cooling processes were explored. Firstly, during the photopolymerization to prepare the LCE, the β-cyano-OPV dye could also absorb the UV light to undergo a photoisomerization as already discussed above and ESI (section 3). Nevertheless, we have shown that the isomerized structures are thermally stable. This indicated that the isomer structures in the LCE micropillars will not be affected during the thermally-induced deformation process. Thus, the observed PL intensity variations do not come from a phenomenon related to a change in the isomerization ratio.

Photo-bleaching is another phenomenon that could induce the decrease of PL intensity. It is related to the photochemical destruction of the fluorophore, which, if present, might also prohibit to perform long observations of our samples by fluorescence microscopy of our samples. We have recorded the PL intensities of the micropillars containing 1 mol% β-cyano-OPV at 25 °C as a function of illumination time until 65 min under UV light (the 365 nm) and under blue light (450 nm) with the same intensities as those used in other experiments presented in this work. The data presented in Fig 7 show that PL intensity remained stable during more than 1h of illumination. This result suggests that the photo-bleaching can be ignored in our experiments.

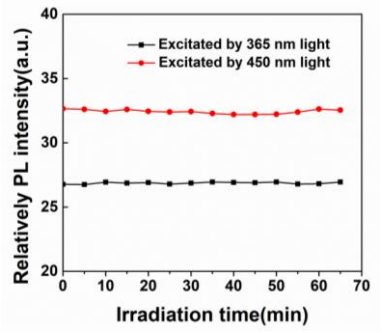

Fig 7. The PL intensity evolution of micropillars containing 1 mol% β-cyano-OPV at 25 °C under the continuous 365 nm UV light and 450 nm blue light illumination.

Now we discuss one by one the effect on the PL intensities of the three main physical parameters occurring within the temperature range 80 – 100 °C on the PL intensities: the temperature change, the nematic-to-isotropic phase transition and the deformation of the micropillars.

In order to study the fluorescence sensitivity to a simple temperature variation, we specially fabricated new micropillars containing 1 mol% β-cyano-OPV but a high concentration of whole crosslinkers (35 mol% in total) which was photopolymerized in the isotropic phase. These pillars were not monodomain with aligned mesogens and were densely crosslinked, so that they would not exhibit any thermomechanical effect since they are some kind of polydomain thermosets. The POM of the highly crosslinked micropillars showed a very weak birefringence, as compared to the lightly crosslinked micropillars (Fig S18). Moreover, only one broad peak was observed in the DSC curve (Fig S19), which was ascribed to the glass-to-isotropic phase transition. The PL intensity and the size of these highly crosslinked micropillars were monitored during a heating-cooling cycling process, from 25 °C to 115 °C. Firstly these micropillars did not change shape and size (Fig S20). Then, as shown in Fig 8, the PL intensity decrease and recovery during the heating and cooling cycle were smooth without abrupt change with temperature increasing under UV or blue light excitations (more changes were observed under blue light excitation). Thus, a simple effect of temperature cannot explain the sharp PL intensity variation for the LCE micropillars, as reported in Fig 6.

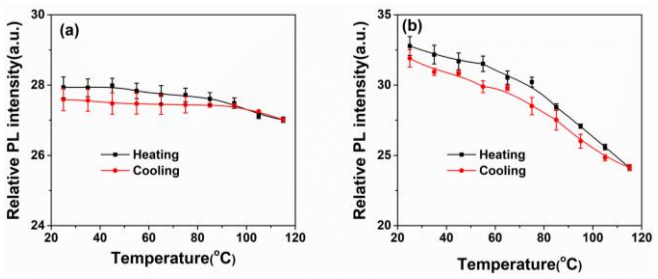

Fig. 8 The PL intensity variation with temperature increasing for the highly crosslinked micropillars containing 1 mol% β-cyano-OPV crosslinker under UV light excitations (a) and under blue light excitation (b).

The "natural" decrease of the PL intensity with the temperature can be then deducted from the global variation traced in the Figure 6, leading to the results presented in the Fig 9. The PL intensity variations depend now only on the deformation process and on the phase transition.

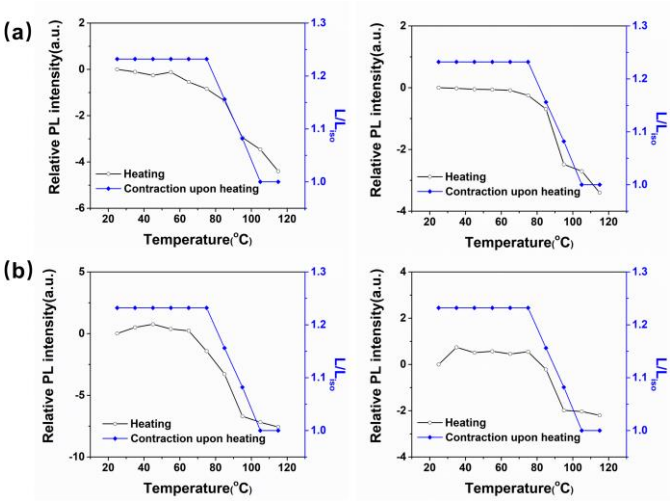

Fig. 9 The PL intensity variation after removing the pure temperature effect during the heating and cooling process under the UV light excitation (a) and under the blue light excitation (b).

In order to further study the relative influences of the deformation process and the nematic-to-isotropic phase transition on the PL intensity variation, we built a new experiment. We studied the evolution of the PL intensity as a function of the temperature for an unpolymerized mixture containing the LC monomer, the flexible crosslinker and the β-cyano-OPV crosslinker, but without the photoinitiator. The observed PL intensity variations will reflect only the evolution connected with the phase transition (nematic-to-isotropic). As shown in the Fig 10a, the PL intensity decreased with the temperature increase. In the Fig 10b, the PL intensity variation for the mixture and its DSC curve are grouped, demonstrating that the sharp decrease in PL intensity is concomitant with the nematic-to-isotropic phase transition at 70-80°C. We also checked out that the PL intensity of the pure β-cyano-OPV in the solid state was not sensitive to temperature in the studied range (see Fig S21). We could conclude that the PL intensity

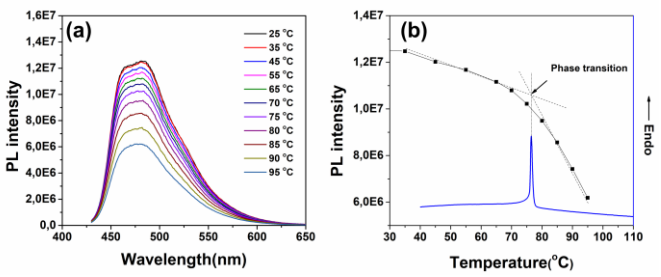

Fig. 10 (a) The fluorescence emission spectra evolution with temperature for the LC monomers mixture containing 1 mol % β-cyano-OPV crosslinker under excitation light at the 420 nm. (b) The PL intensity variation at λ_{em} = 481 nm and the DSC curve of the unpolymerized mixture upon heating.

variation observed for the monomers mixture was caused by the phase transition.

At last, the evolution of the emission spectra with the concentration of β-cyano-OPV crosslinker in micropillars was investigated. As shown in Fig 11a, when the concentration of the dye was 0.5 mol%, the maximum emission spectra had peak value at 476 nm, while for a 5 mol% concentration, the emission peak had a limited red shift to 492 nm. Meanwhile, the variation of the emission spectra with the temperature change was also explored to check the state of the β-cyano-OPV molecules during the deformation process. As seen in Fig 11b, the PL intensity decreased with the temperature increasing. However, the emission spectra did not show any shift and curve shape change up to the isotropic temperature, which means that the β-cyano-OPV molecules always remained in the "monomer state" during the deformation process. Similar results were obtained for the micropillars with different β-cyano-OPV concentrations (Fig S22). This might be linked with the relative small contraction observed for the LCE micropillars, which prevented the dye molecules to come close enough to each other to build effective aggregates and to behave as excimers.

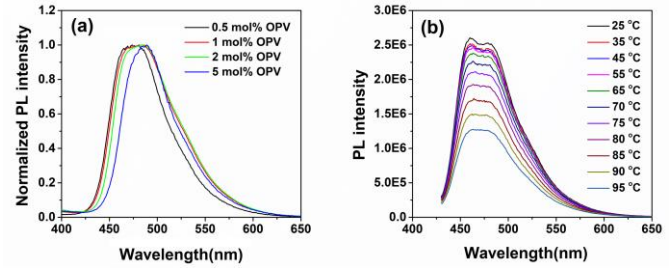

Fig. 11 (a) The fluorescence emission spectra of the micropillars with different content of β-cyano-OPV. (b) The thermally-induced PL intensity variation for micropillars containing 1 mol% β-cyano-OPV.

After these careful analyses of factors that might affect the PL intensity of LCE micropillars, we can conclude that the PL intensity variation observed for the micropillars was caused by the phase transition and the temperature change. The N-I phase transition was the major reason of the abrupt decrease of PL intensity of LCE micropillars during thermal-mechanical deformation, while the temperature increase caused only a

smooth decrease of PL intensity. This is comprehensible from the principle of fluorescence. A part of the energy of the excited state of monomeric β-cyano-OPV was annihilated by radiation, leading to the fluorescence. Upon heating and especially in isotropic phase above T_{NI}, the β-cyano-OPV molecule gained more freedom of inter- and intra-molecular motions. These molecular motions deactivated more efficiently its excitons in non-radiative manners. Consequently, the part of radiative channel to decay the energy of the excited state became less efficient, and then the fluorescence emission of the micropillars was weakened.

Conclusion

We prepared new nematic LCE micropillars by including a fluorescent dye (β-cyano-OPV) in the crosslinker. The quantum yield of the fluorescent LCE was 85% ± 10% as measured by using the integrating sphere method. The potential factors which might affect the photoluminescence intensity during the heating and cooling cycling process were investigated in detail. The nematic-to-isotropic phase transition of the LCE micropillars has the greatest effect on the PL intensity variations. Meanwhile, during the deformation process, no obvious shift of the fluorescence emission spectra could be detected. We concluded that the β-cyano-OPV dye molecules stayed in the monomeric state during the deformation process of LCE micropillars with the contraction (expansion) ratio L/L_{iso} of 1.25. The study of fluorescent LCEs presenting higher contraction ratio are in progress in order to get excimers and shift of the fluorescence emission spectra. The present work might provide a potential protocol to develop LCE fluorescent sensors and might have potential application in dynamic display device.

Experimental section

Characterization

1H NMR and 13C NMR spectra were recorded on Bruker Avance 400 MHz spectrometer at 297 K. Deuterated chloroform ($CDCl_3$) was used as the solvent and TMS (tetramethylsilane) was used as the internal reference. Calorimetric measurements of LC monomers and elastomers were performed using a Perkin Elmer DSC7 instrument. The reference cell was kept empty and the sample cell was filled with polymer sample (5 to 10 mg). Samples were scanned over a temperature range between 25 °C and 120 °C with a scanning rate of 10 °C/min. Thermogravimetric analysis (TGA) of the elastomer containing β-cyano-OPV crosslinker was carried out on SDT Q600 TA instrument. The sample (5-10 mg) was measured under a nitrogen atmosphere over the temperature range of 25 to 700 °C with a heating rate of 20 °C/min. The fluorescence emission spectroscopy characterization was carried out on a FluoroMax spectrofluorometer. The fluorescence quantum yield was measured on spectrofluorometer Fluorolog FL3-221 from Horiba Jobin-Yvon, equipped with a Horiba Jobin-Yvon integration sphere accessory. PL dyes samples were dissolved in the dichloromethane (DCM). Fluorescence emission spectroscopy of the LCE micropillars was carried out on the same FluoroMax spectrofluorometer. The LCE micropillars were dispersed in low viscosity silicone oil in a 0.2 cm thickness quartz cell. UV–Vis spectra were obtained with a PerkinElmer Lambda 800 instrument. The PL dye was dissolved in dichloromethane (DCM) to obtain the spectra in solution. The PL intensity variations were measured by fluorescence microscopy. Samples were observed directly via a Leica DMIL LED Fluo inverted microscope equipped with a Linkam heating stage. The excitation light was supplied by a Cool LED system (pE-300 white, Leica). For the UV light excitation, the fluorescence filter cube of DAPI was used (excitation wavelength between 325-375 nm, emission wavelength between 435-485 nm). For the blue light excitation, the fluorescence filter cube of GFP was used (excitation wavelength between 450-490 nm, emission wavelength between 500-550 nm). Polarizing microscopy (POM) observations were obtained on a Motic BA310POL equipped with a Motic CCD camera, and a Mettler FP 80 hot stage.

Fabrication of the micropillars

Poly(dimethylsiloxane) (PDMS) molds were prepared via photo-lithography and soft-lithography steps[47]. Multiple mixtures were prepared from the monomer MA444 ((4-methacryloyloxy)butyl 2,5-di-(4'-butyloxybenzoyloxy) benzoate), the flexible crosslinker (1,6-hexanediol dimethacrylate) and the β-cyano-OPV crosslinker ((((1Z,1'Z)-1,4-phenylenebis(1-cyanoethene-2,1-diyl))bis(4,1-phenylene))bis(oxy))bis(hexane-6,1-diyl) bis(2-methylacrylate)), and the photoinitiator (Iragure 369, (2-benzyl-2-(dimethylamino)-4'-morpholinobutyrophenone). The concentration of the photoinitiator was kept at 2 mol%, while various ratios of monomer/flexible-crosslinker/OPV-crosslinker have been tested.

The micron-sized LCE pillars were fabricated as previously described[14]. The mixture of LC monomer, flexible and fluorescent crosslinkers, and photo-initiator were deposited on a glass coverslip placed atop a permanent magnet (~1 T NdFeB rare earth magnet) in a heating stage. Then the mixture was heated up to its isotropic phase (100 °C). A soft PDMS mold was gently pressed onto the melted mixture to force the mixture to fill the inner structure of the mold. The monomers mixture was then cooled down to its nematic phase (60 °C) at a slow rate (1 °C/ min). During the cooling process, the magnetic field aligns the nematic phase with the nematic director pointing along the long axis of the pillars. During the process, an oxygen-free environment was kept by placing the setup in a zip-lock bag flushed with a slow stream of argon. A 365 nm UV light source (30mW/cm^2) was used to initiate the photopolymerization for 30 minutes. After the sample was cooled down to room temperature, the PDMS mold was peeled off to leave a regular array of micropillars. A sharp razor blade was used to untie the micropillars from the glass

surface. The free micropillars were suspended in low viscosity silicone oil.

PL intensity measurement of the micropillars

The relative PL intensity variations for the micropillars were measured using Image J software. Keeping the same exposition time (40 ms), gain (2%), Gamma (1) parameters of the fluorescence microscope, the fluorescence images at different temperatures were recorded. The captured fluorescence images were imported in Image J, and changed to an 8-bit grayscale mode. Recording the sum of grayscale values of a fluorescent micropillar in its whole area gave us the relative fluorescence intensity of a micropillar. Ten micropillars were analysed for each experiment to give the average value.

Conflicts of interest

There are no conflicts to declare.

Acknowledgements

This work has received the support from the French National Research Agency (ANR-16-CE29-0028) and from the "Institut Pierre-Gilles de Gennes" (IPGG, laboratoire d'excellence, "Investissements d'avenir" programs ANR-10-IDEX-0001-02 PSL, ANR10-LABX-31 and ANR-10-EQPX-34). Bin NI gratefully acknowledges the China Scholarship Council for funding his PhD scholarship. We thank Guylaine Ducouret, Mohamed Hanafi and Rémi Métivier for their help in TGA analysis and quantum yield measurement.

Notes and references

1. E.-K. Fleischmann and R. Zentel, *Angew. Chem. Int. Ed.*, 2013, **52**, 8810-8827.
2. K. M. Lee, M. L. Smith, H. Koerner, N. Tabiryan, R. A. Vaia, T. J. Bunning and T. J. White, *Adv. Funct. Mater.*, 2011, **21**, 2913-2918.
3. A. H. Gelebart, D. Jan Mulder, M. Varga, A. Konya, G. Vantomme, E. W. Meijer, R. L. B. Selinger and D. J. Broer, *Nature*, 2017, **546**, 632-636.
4. M. Chen, X. Xing, Z. Liu, Y. Zhu, H. Liu, Y. Yu and F. Cheng, *Appl. Phys. A*, 2010, **100**, 39-43.
5. E.-K. Fleischmann, H.-L. Liang, N. Kapernaum, F. Giesselmann, J. Lagerwall and R. Zentel, *Nat. Comm.*, 2012, **3**, 1178.
6. H. Modler and H. Finkelmann, *Berichte der Bunsengesellschaft für physikalische Chemie*, 1990, **94**, 836-856.
7. M.-H. Li, P. Keller, B. Li, X. Wang and M. Brunet, *Adv. Mater.*, 2003, **15**, 569-572.
8. M.-H. Li, P. Keller, J. Yang and P.-A. Albouy, *Adv. Mater.*, 2004, **16**, 1922-1925.
9. E. M. T. Mark Warner, *Oxford University Press*, 2003.
10. M. H. Li, A. Brûlet, P. Davidson, P. Keller and J. P. Cotton, *Phys. Rev. Lett.*, 1993, **70**, 2297-2300.
11. J. P. Cotton and F. Hardouin, *Prog. Polym. Sci.*, 1997, **22**, 795-828.
12. D. J. Broer, J. Boven, G. N. Mol and G. Challa, *Die Makromolekulare Chemie*, 1989, **190**, 2255-2268.
13. H. Yang, A. Buguin, J.-M. Taulemesse, K. Kaneko, S. Méry, A. Bergeret and P. Keller, *J. Am. Chem. Soc.*, 2009, **131**, 15000-15004.
14. A. Buguin, M.-H. Li, P. Silberzan, B. Ladoux and P. Keller, *J. Am. Chem. Soc.*, 2006, **128**, 1088-1089.
15. S. Schuhladen, F. Preller, R. Rix, S. Petsch, R. Zentel and H. Zappe, *Adv. Mater.*, 2014, **26**, 7247-7251.
16. C. Ohm, C. Serra and R. Zentel, *Adv. Mater.*, 2009, **21**, 4859-4862.
17. L. Liu, M.-H. Liu, L.-L. Deng, B.-P. Lin and H. Yang, *J. Am. Chem. Soc.*, 2017, **139**, 11333-11336.
18. Y. Xia, X. Zhang and S. Yang, *Angew. Chem. Int. Ed.*, 2018, **57**, 5665-5668.
19. Y. Xia, G. Cedillo-Servin, R. D. Kamien and S. Yang, *Adv. Mater.*, 2016, **28**, 9637-9643.
20. Z. Pei, Y. Yang, Q. Chen, E. M. Terentjev, Y. Wei and Y. Ji, *Nat. Mater.*, 2013, **13**, 36.
21. T. H. Ware, M. E. McConney, J. J. Wie, V. P. Tondiglia and T. J. White, *Science*, 2015, **347**, 982-984.
22. Z. L. Wu, Z. J. Wang, P. Keller and Q. Zheng, *Macromol. Rapid Commun.*, 2016, **37**, 311-317.
23. X. Liu, R. Wei, P. T. Hoang, X. Wang, T. Liu and P. Keller, *Adv. Funct. Mater.*, 2015, **25**, 3022-3032.
24. F. Ge, R. Yang, X. Tong, F. Camerel and Y. Zhao, *Angew. Chem. Int. Ed.*, 2018, **57**, 11758-11763.
25. H. Zeng, O. M. Wani, P. Wasylczyk, R. Kaczmarek and A. Priimagi, *Adv. Mater.*, 2017, **29**, 1701814.
26. Y. Yu, M. Nakano and T. Ikeda, *Nature*, 2003, **425**, 145.
27. M. Wang, B.-P. Lin and H. Yang, *Nat. Comm.*, 2016, **7**, 13981.
28. T. Ube, K. Kawasaki and T. Ikeda, *Adv. Mater.*, 2016, **28**, 8212-8217.
29. J. J. Wie, M. R. Shankar and T. J. White, *Nat. Comm.*, 2016, **7**, 13260.
30. S. Courty, J. Mine, A. R. Tajbakhsh and E. M. Terentjev, *Europhys. Lett.*, 2003, **64**, 654-660.
31. K. Urayama, S. Honda and T. Takigawa, *Macromolecules*, 2005, **38**, 3574-3576.
32. S. Hashimoto, Y. Yusuf, S. Krause, H. Finkelmann, P. E. Cladis, H. R. Brand and S. Kai, *Appl. Phys. Lett.*, 2008, **92**, 181902.
33. A. Agrawal, H. Chen, H. Kim, B. Zhu, O. Adetiba, A. Miranda, A. Cristian Chipara, P. M. Ajayan, J. G. Jacot and R. Verduzco, *ACS Macro Lett.*, 2016, **5**, 1386-1390.
34. A. Pucci, F. Di Cuia, F. Signori and G. Ruggeri, *J. Mater. Chem.*, 2007, **17**, 783-790.
35. H. Sasabe, N. Toyota, H. Nakanishi, T. Ishizaka, Y.-J. Pu and J. Kido, *Adv. Mater.*, 2012, **24**, 3212-3217.
36. Y.-T. Lee, C.-L. Chiang and C.-T. Chen, *Chem. Commun.*, 2008, 2, 217-219.
37. D. W. R. Balkenende, S. Coulibaly, S. Balog, Y. C. Simon, G. L. Fiore and C. Weder, *J. Am. Chem. Soc.*, 2014, **136**, 10493-10498.
38. T. Han, J. W. Y. Lam, N. Zhao, M. Gao, Z. Yang, E. Zhao, Y. Dong and B. Z. Tang, *Chem. Commun.*, 2013, **49**, 4848-4850.
39. X. Hou, C. Ke, C. J. Bruns, P. R. McGonigal, R. B. Pettman and J. F. Stoddart, *Nat. Comm.*, 2015, **6**, 6884.
40. C. Löwe and C. Weder, *Adv. Mater.*, 2002, **14**, 1625-1629.
41. B. R. Crenshaw and C. Weder, *Chem. Mater.*, 2003, **15**, 4717-4724.
42. R. Wei, Y. He, X. Wang and P. Keller, *Macromol. Rapid Commun.*, 2014, **35**, 1571-1577.
43. Z. Liang, E. Sun, S. Pei, L. Li, F. Qin, Y. Zheng, H. Zhao, Z. Zhang and W. Cao, *Opt. Express*, 2016, **24**, 29209-29215.

44. Y. Yılmaz, *Physical Review E*, 2002, **66**, 052801.
45. G. Baur, A. Stieb and G. Meier, *J. Appl. Phys.*, 1973, **44**, 1905-1906.
46. M.-H. Li, P. Keller, E. Grelet and P. Auroy, *Macromol. Chem. Phys.*, 2002, **203**, 619-626.
47. D. C. Duffy, J. C. McDonald, O. J. A. Schueller and G. M. Whitesides, *Anal. Chem.*, 1998, **70**, 4974-4984.